

# Hot isostatic pressing of Y-TZP powder compacts

J.-Y. KIM, S. OKAMOTO, N. UCHIDA, K. UEMATSU

*Faculty of Engineering, Nagaoka University of Technology, Kamitomioka, Nagaoka, Niigata, 940-21 Japan*

A fundamental study of hot isostatic pressing (HIPing) was performed on Y-TZP powder compacts, and the effect of the various HIPing process variables (time, temperature and pressure) was examined on the densification behaviour. The results were analysed using Ashby's HIPing model, which was found to be applicable for this system. The densification was found to be governed by the grain-boundary diffusion of cations. The use of grain-boundary transport characteristics determined in this study enabled HIP maps to predict the densification behaviour of HIPing within an accuracy of a factor of three for all stages of densification, except for the results at low HIPing pressure and the region of near full density.

## 1. Introduction

Considerable attention has been paid to  $Y_2O_3$ -doped tetragonal  $ZrO_2$  polycrystals (Y-TZP) because of their excellent mechanical properties [1-5]. In the last few years the application of the hot isostatic pressing (HIPing) to these materials has been studied extensively [6-8]. The process has potential for the fabrication of high-performance ceramics, but very little appears to be known of the fundamentals of HIP densification for these materials.

Recently, Helle *et al.* [9] studied the HIPing process, and proposed the concept of HIP maps. The map identifies the dominant mechanism of densification (plastic yielding, power-law creep or diffusional densification, etc.) and predicts the density reached under given HIPing conditions. Good agreement was found between the theoretical prediction and the experimental results in the high-density region of the final stage of sintering for  $Al_2O_3$ . Extensive tests remain on the model for more materials and also for a wider density region. The model also assumes the grain size to be constant, so that grain growth was ignored.

More recently, Uematsu *et al.* [10, 11] examined the densification behaviour of HIPing over all stages of sintering using  $Al_2O_3$  as a model material. After analysing the results using Ashby's HIPing model, they concluded that if grain growth is properly taken into account, the map can predict the density after HIPing with high accuracy.

The purpose of the present study was to examine the densification behaviour of Y-TZP powder compacts during HIPing. The study included (1) the effect of various HIPing conditions and characteristics of the powder compacts on densification, and (2) further examination of Ashby's model.

## 2. Experimental procedure

Three kinds of commercial 3 mol %  $Y_2O_3$ -doped  $ZrO_2$

powders TZ-3YA, TZ-3YS, Tosoh Co. Ltd, Tokyo; HSY-3.0 S.D., Daiichi Kigenso Kagaku Kogyo Co. Ltd., Osaka) were used as starting materials. As-received powders were formed into pellets (14 mm diameter by 8 mm long) at 20 MPa, and then isostatically pressed at 200 MPa. In case of the spray-dried powders, the powder compact binders were burned out by heating them at  $1^\circ C min^{-1}$  to  $800^\circ C$ , and by holding at this temperature for 2 h in air. After the pellets were coated with BN powder to prevent reaction with the capsule material, they were put into a cylindrical capsule made of pyrex glass, evacuated at  $700^\circ C$  for 1 h, and sealed. The capsule was placed inside commercial HIPing apparatus (Model QIH-9, NKK-ASEA, Tokyo) and heated ( $10^\circ C min^{-1}$ ) to the softening temperature of pyrex glass ( $850^\circ C$ ) in vacuum. Pressure was then applied and the capsule heated again to final temperature at the same rate. The starting point of HIPing was taken at the point where the temperature and pressure had reached the desired values. HIPing conditions of the present work were (1) 1000 to  $1200^\circ C$ ; (2) 5 to 200 MPa; and (3) 0.5 to 4 h. After HIPing, the specimens were cooled in the apparatus, removed from the capsule, and ground to remove surface contamination. The densities of the HIPed specimens were measured by the Archimedes' method. The microstructure was examined on polished and thermally etched surfaces using a scanning electron microscope (model JSM-T100, Jeol, Tokyo).

## 3. Results

Fig. 1 shows the effect of HIPing temperature on the densification of various powder compacts at 50 MPa for 1 h. The densities increased with HIPing temperature for all specimens. No powder can achieve full density below  $1200^\circ C$  but all powders can reach almost full density at  $1200^\circ C$ . Specimens of TZ-3YA

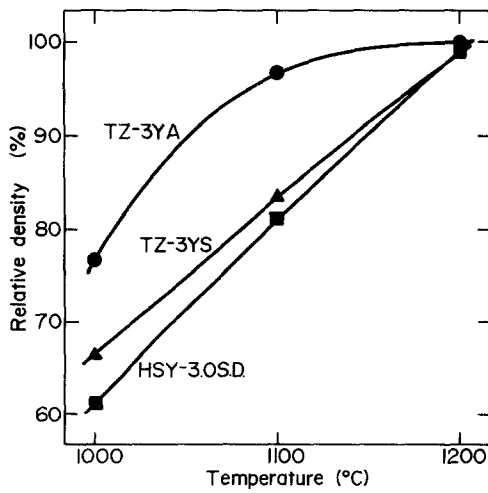


Figure 1 Effect of HIPing temperature on the densification of various powder compacts at 50 MPa for 1 h.

have higher densities than the other specimens for all conditions.

Fig. 2 shows the effect of HIPing time on the densification of various powder compacts at 1200°C and 50 MPa. The densities increased with HIPing time for all specimens. Specimens of TZ-3YA can achieve almost full density for any condition. Specimens of TZ-3YS and HSY-3.0 S.D. can achieve almost full density after 1 h. Their densities, however, increased slightly for 4 h.

Fig. 3 shows the effect of HIPing pressure on the densification of various powder compacts at 1200°C for 1 h. The densities increased with HIPing pressure for all specimens. No powder can achieve full density at 5 MPa. All powders can reach almost full density at 50 and 200 MPa. Specimens of TZ-3YA again had higher densities than the others for all conditions.

Fig. 4 shows the microstructures of specimens at various stages of densification. Grain sizes increased slightly with increasing densities. Larger grains were found in the specimens having higher densities. Clearly, grain growth occurred with densification during HIPing.

Fig. 5 shows a quantitative relationship between grain size and the relative density for all specimens. Most of the data represent results obtained at 50 MPa.

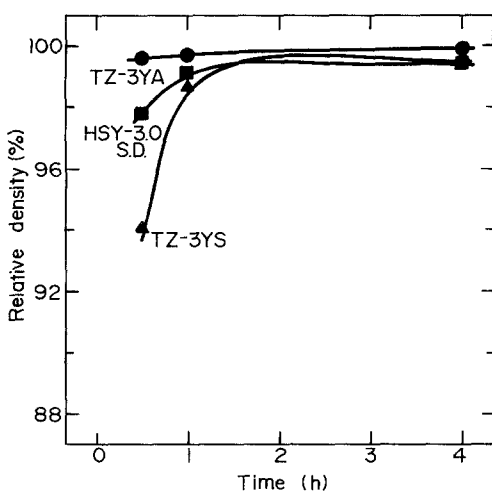


Figure 2 Effect of HIPing time on the densification of various powder compacts at 1200°C and 50 MPa.

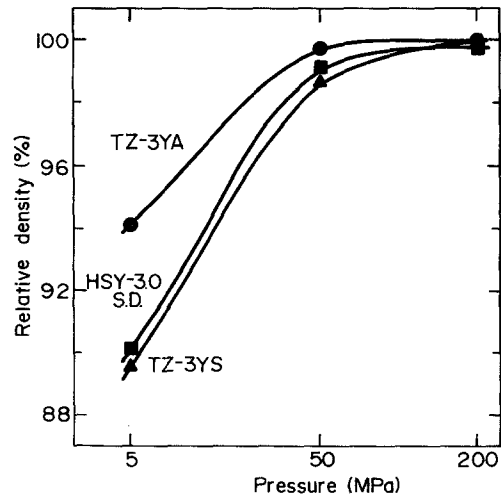


Figure 3 Effect of HIPing pressure on the densification of various powder compacts at 1200°C for 1 h.

The results obtained at 5 and 200 MPa are also included. The grain growth started at a relative density of approximately 80%, and became significant above 95%.

#### 4. Discussion

Both grain growth and densification occurred during HIPing. Grain growth is known to reduce the densification rate [12], and therefore must be understood before any detailed analysis is possible.

Fig. 6 shows the relation between the grain size and porosity for HIPed specimens. An approximate linear relationship exists between logarithms of grain size and porosity for all specimens. This relationship suggests that the equation proposed by Kuczynski [13] is applicable for these cases, i.e.

$$GP^n = m \quad (1)$$

where  $G$  is the grain size,  $P$  the porosity and  $m$  a constant which varied with several powders. The values of  $n$  also varied slightly with the type of powder in this study. This result is similar to that reported for  $Al_2O_3$  [11]. The variation of these values with the type of powder can be attributed to the different particle size distributions of the starting powders and the resultant minor differences in microstructural characteristics.

Apart from the detailed mechanism involved in the grain growth, an empirical equation which can express the relationship between the porosity and the grain size for general cases may be important from the practical point of view. To obtain the values of  $n$  and  $m$ , the constant  $n$  in the above expression was assumed to have the same value for all cases. A least squares analysis gave the best value of  $1/23$  for  $n$  in HIPed specimens.

The experimental results for the HIPing process are analysed using Ashby's HIPing model. In the model, the densification process consisted of two stages; an initial stage where necks grow at the contact points, and a final stage where isolated residual pores shrink. Through all stages it was found that the densification occurred by plastic yielding, power-law creep, or by diffusion. The total rate of densification was given by summing the densification rate for each process. The

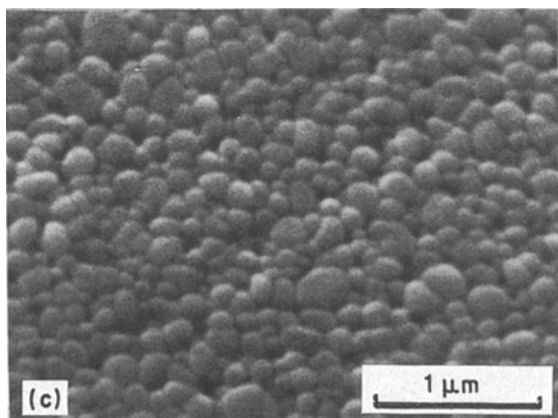
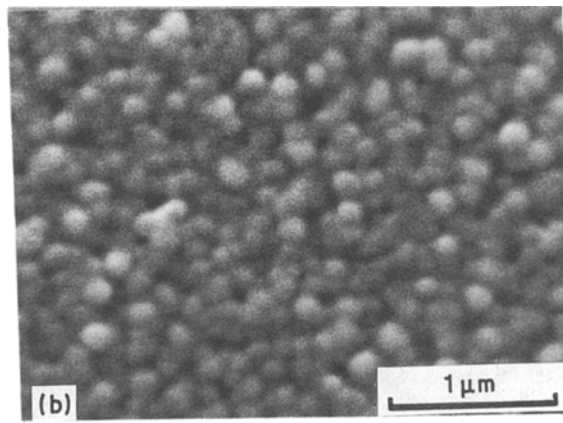
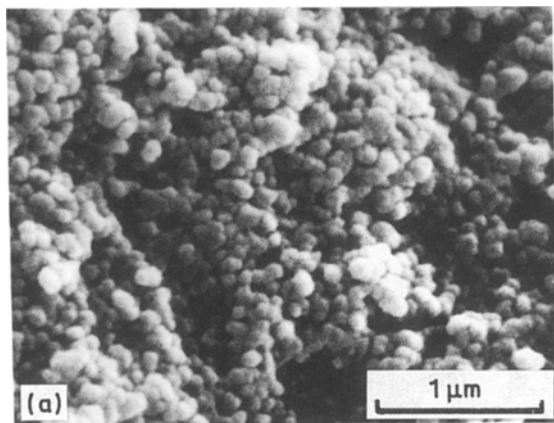


Figure 4 Scanning electron micrographs of specimens of TZ-3YA HIPed under various conditions. (a) 1000°C, 50 MPa, 1 h; (b) 1100°C, 50 MPa, 1 h; (c) 1200°C, 50 MPa, 1 h.

current density could be calculated as functions of time, temperature, pressure, initial grain size and initial relative density, using several material data relevant to densification behaviour.

In this study, the Runge-Kutta method was used for solving the rate equation of densification. In defining the initial conditions, the grain size of specimens HIPed at 1000°C, 50 MPa for 1 h was chosen as the initial grain size of the powder compacts. The values of particle size measured by other methods, such as BET, centrifugal sedimentation and light scattering methods, involve significant uncertainty, and are inadequate to define effective particle size relevant to the densification process. In the initial stage of sintering, little grain growth occurs with densification, as shown in Fig. 5. The grain size of a specimen having

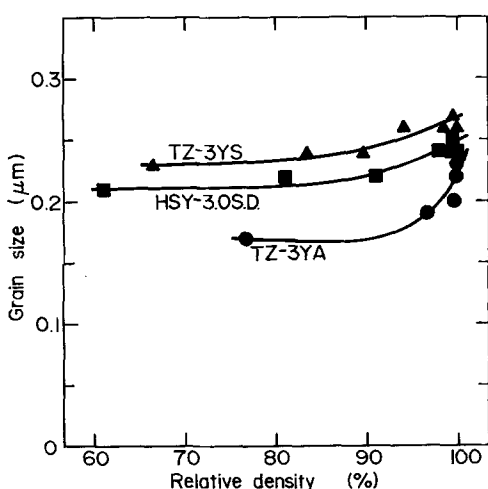


Figure 5 Change of grain size with densification during HIPing for all specimens.

the minimum density after HIPing is believed to be approximately the same as the initial grain size of the powder compacts. Furthermore, analysis and experiment show that densification up to 60% theoretical density is completed almost instantaneously for most conditions, and the errors of densification time introduced in this early stage of densification does not affect the overall analysis. The grain sizes expressed by the Equation 1 with specific constants  $n$  were used to express the grain sizes for the density above 80% in solving the rate equation of densification. The material data used for constructions of HIP maps are listed in Table I. Through constructions of HIP maps, we found that the contribution of grain-boundary diffusion of cations was dominant over other mechanisms, and densification was assumed to be governed by the grain-boundary diffusion of cations at all conditions for all specimens.

Fig. 7 shows the ratio of HIPing time required experimentally ( $t_{exp}$ ) to that predicted by theory ( $t_{theory}$ ) to achieve current densities for all specimens. The ratio was found to be systematically much larger than unity, and about the range of hundreds. Rather constant deviation of the experiment from the theory, however, suggests that the concept of the HIP map is fundamentally correct, and is applicable for expressing

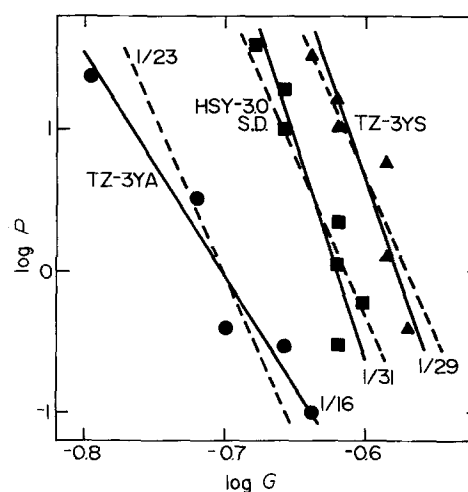


Figure 6 Relation between logarithm of porosity and logarithm of grain size for all specimens.

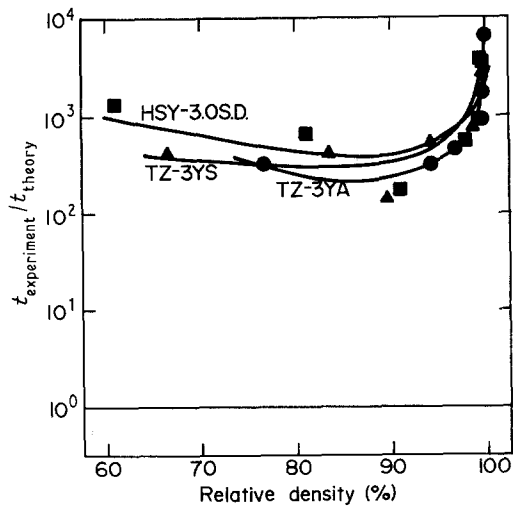


Figure 7 The ratio of experimental to theoretical HIPing time required to achieve current densities. Theoretical data are calculated using the diffusion coefficients proposed by Oishi *et al.* [18].

the densification behaviour during HIPing, if material data are revised.

One clear source for the above disagreement between theory and experiment is the diffusion coefficient applied for the analysis. The previously obtained diffusion coefficients [18] applied for the present analysis were clearly inadequate. Grain-boundary diffusion coefficient times grain boundary width,  $\delta D_b$ , applied for this analysis was determined for stabilized zirconia doped with 16 mol %  $Y_2O_3$ , having an average grain radius of about  $30 \mu m$  for the temperature range 1584 to 2116°C. In contrast, this study used tetragonal zirconia polycrystals doped with 3 mol %  $Y_2O_3$  having an average grain radius of about  $0.1 \mu m$ . The temperature range studied was 1000 to 1200°C.

Fig. 8 shows the grain-boundary diffusion coefficient times grain boundary width determined in this study to give the best fit between the theory and the experiment. The data obtained at 5 MPa were excluded for

TABLE I Material data used for the construction of HIP maps

Material property	Data	Reference
Atomic volume, $\Omega$ ( $m^3$ )*	$3.36 \times 10^{-29}$	[14]
Burger's vector, $b$ (m)*	$5.1 \times 10^{-10}$	[14]
Melting temperature, $T_m$ (K)	2985	[15]
Yield strength, $\sigma_y$ (MPa)†	4000	[16]
Shear modulus‡		
at 300 K, $u_0$ (MPa)	$9.6 \times 10^4$	[17]
$T_m/u_0 du/dT$	-0.8	
Grain-boundary diffusion		
$D_{ob}$ ( $m^3 sec^{-1}$ )	$1.5 \times 10^{-12}$	[18]
$Q_b$ ( $kJ mol^{-1}$ )	309	
Volume diffusion		
$D_{ov}$ ( $m^2 sec^{-1}$ )	$3.1 \times 10^{-6}$	[18]
$Q_v$ ( $kJ mol^{-1}$ )	391	
Power-law creep		
$n$	2	[19]
$A$ (Dorn constant)§	$5 \times 10^{-4}$	[20]

\*From lattice parameters given by Tsukuma *et al.* [14].

†Using room-temperature yield strength instead of data for the temperature dependence of the yield strength, because the data were difficult to find.

‡Taken from graphic data given by Lynch *et al.* [19].

§Inferred from relations between  $n$  and  $A$  given by Stocker and Ashby [20].

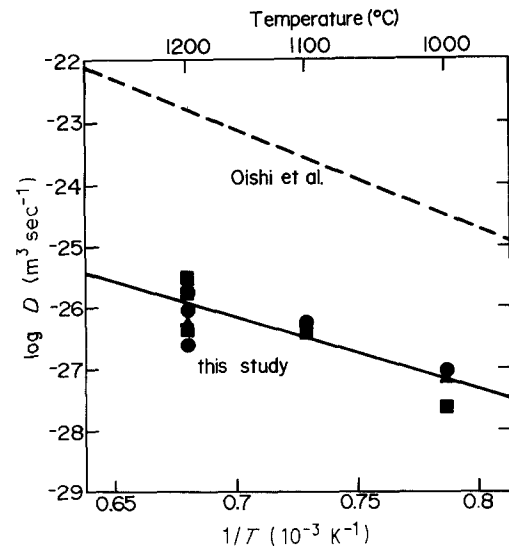


Figure 8 Grain-boundary diffusion parameters for Y-TZP determined in this study as a function of temperature. The value proposed by Oishi *et al.* [18] is also presented for comparison. (●) TZ-3YA, (▲) TZ-3YS, (■) HSY-3.0 S.D.

the reason explained later. The diffusion coefficients were calculated using simple regression analysis, and are expressed by Equation 2.

$$\delta D_{ob} = 7.1 \times 10^{-19} \exp(-220 \text{ kJ mol}^{-1}/RT) \text{ m}^3 \text{ sec}^{-1} \quad (2)$$

In the temperature range studied, the present diffusion coefficients were approximately three orders of magnitude smaller than those extrapolated from high-temperature data [18]. A much smaller pre-exponential term is mainly responsible for this result. The activation energy of this study is approximately equal to that of the previous study.

In Figs 9 and 10, experimental data were presented in HIP maps constructed with the diffusion coefficients determined in this study. The experimental results were well expressed by the HIP maps. The use of the diffusion coefficients determined in this study enabled us to express the densification behaviour of Y-TZP with high accuracy. Note, however, that the

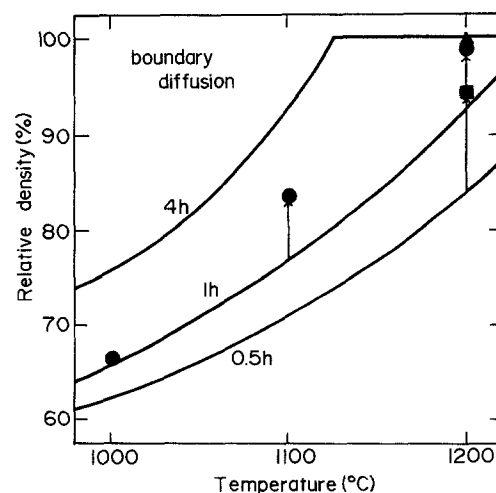


Figure 9 HIP map for TZ-3YS showing the relation between the density, temperature and time, calculated using the diffusion coefficients determined in this study.  $P = 50 \text{ MPa}$ ,  $d = 0.23 \mu m$ ,  $D_0 = 48\%$ . Experimental results: (■) 0.5 h; (●) 1 h; (▲) 4 h.

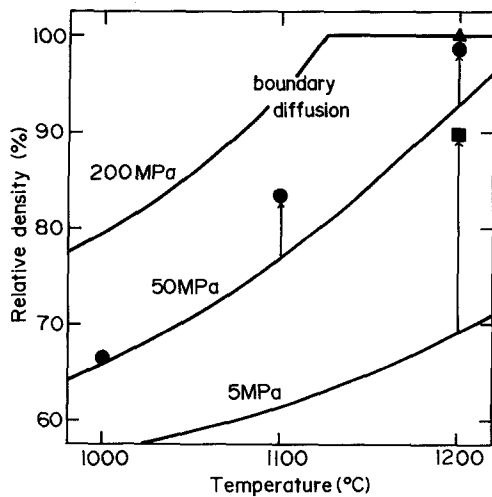


Figure 10 HIP map for TZ-3YS showing the relation between the density, temperature and pressure, calculated using the diffusion coefficients determined in this study.  $t = 1$  h,  $d = 0.23 \mu\text{m}$ ,  $D_0 = 48\%$ . Experimental results: (■) 5 MPa; (●) 50 MPa; (▲) 200 MPa.

disagreement between theory and experiment is high for the 5 MPa results. We feel that the driving force by surface curvature is also not negligible for this case. A rough estimate of the pressure generated by a curvature of  $\sim 0.1 \mu\text{m}$ , is 20 MPa.

Fig. 11 shows the revised ratios of HIPing time required experimentally ( $t_{\text{exp}}$ ) to that predicted by theory ( $t_{\text{theory}}$ ) to achieve current densities for all specimens. The diffusion coefficients determined in this study were used for this analysis. The line at unity represents the complete agreement between the theory and the experiment. Most of the results which deviate markedly from unity are either those at low HIPing pressure or those near full densities. The former involves errors as explained above, and the latter inherently has a large uncertainty due to the errors

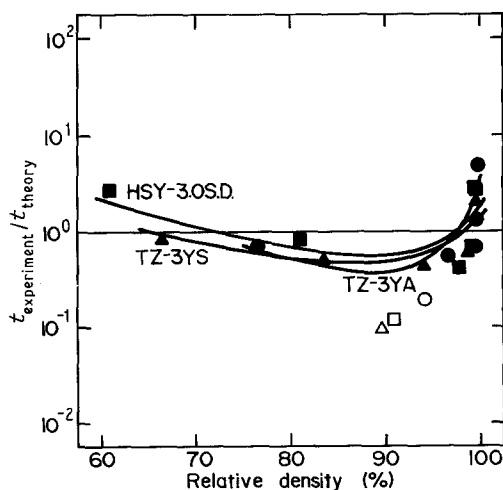


Figure 11 The ratio of experimental to theoretical HIPing time required to achieve current densities. Theoretical data are calculated with the diffusion coefficients determined in this study. (○, □, △) 5 MPa.

associated with the density measurement. With these in mind, in general, the densification behaviour of all specimens can be expressed with reasonable accuracy by the theory.

The results obtained in this study clearly show that Ashby's HIPing model, with grain growth taken into account, can predict the densification of Y-TZP during HIPing within the accuracy of a factor of three for all specimens, except for results at low HIPing pressure and in the region of extremely high density. The good agreement between the model and the experiment shows that the processes during densification are, in fact, as predicted by the model; the densification is governed by the grain-boundary diffusion of cations throughout the process. The grain-boundary diffusion coefficient determined in this study may be quite adequate for the analysis of HIP densification of Y-TZP.

## References

1. T. K. GUPTA, F. F. LANGE and J. H. BECHTOLD, *J. Mater. Sci.* **13** (1978) 1464.
2. F. F. LANGE, *ibid.* **17** (1982) 240.
3. M. RÜHLE, N. CLAUSSEN and A. H. HEUER, in "Advances in Ceramics", Vol. 12, edited by N. Claussen, M. Rühle and A. H. Heuer (American Ceramic Society, Columbus, Ohio, 1984) p. 352.
4. S. SCHMAUDER and H. SCHUBERT, *J. Amer. Ceram. Soc.* **69** (1986) 534.
5. T. SATO and M. SHIMADA, *ibid.* **68** (1985) 356.
6. K. TSUKUMA and M. SHIMADA, *Amer. Ceram. Soc. Bull.* **64** (1985) 310.
7. T. MASAKI, *J. Amer. Ceram. Soc.* **69** (1986) 638.
8. V. GROSS and M. V. SWAIN, *J. Aust. Ceram. Soc.* **22** (1986) 1.
9. A. S. HELLE, K. E. EASTERLING and M. F. ASHBY, *Acta Metall.* **33** (1985) 2163.
10. K. ITAKURA, N. UCHIDA, K. UEMATSU, K. SAITO, A. MIYAMOTO and T. MIYASHITA, *J. Ceram. Soc. Jpn* **96** (1988) 574.
11. K. UEMATSU, K. ITAKURA, N. UCHIDA, K. SAITO, A. MIYAMOTO and T. MIYASHITA, *J. Amer. Ceram. Soc.* **73** (1990) 74.
12. Y. MORIYOSHI and W. KOMATSU, *ibid.* **53** (1970) 672.
13. G. C. KUCZYNSKI, *Mater. Sci. Monogr.* **8** (1981) 44.
14. K. TSUKUMA, Y. KUBOTA and T. TSUKIDATE, in "Advances in Ceramics", Vol. 12, edited by N. Claussen, M. Rühle and A. H. Heuer (American Ceramic Society, Columbus, Ohio, 1984) p. 382.
15. V. S. STUBICAN, R. C. HINK and S. P. RAY, *J. Amer. Ceram. Soc.* **61** (1978) 17.
16. M. F. ASHBY and D. R. H. JONES, in "Engineering Materials, an Introduction to Their Properties and Applications" (Pergamon, Oxford, 1980) p. 78.
17. J. F. LYNCH, D. JOHNSON and J. K. THOMPSON in "Engineering Property Data on Selected Ceramics, Vol. 3, Single Oxides" (Metals and Ceramics Information Center, Battelle Columbus Laboratories, 1981) p. 5.4.5.
18. Y. OISHI, KEN ANDO and Y. SAKKA, in "Advances in Ceramics", Vol. 7, edited by M. F. Yan and A. H. Heuer (American Ceramic Society, Columbus, Ohio, 1983) p. 208.
19. F. WAKAI, S. SAKAGUCHI and Y. MATSUNO, *Adv. Ceram. Mater.* **1** (1986) 259.
20. R. L. STOCKER and M. F. ASHBY, *Scripta Metall.* **7** (1973) 115.

Received 31 May  
and accepted 23 October 1989